Robust Transport Barriers Resulting from Strong Kolmogorov-Arnold-Moser Stability

I. I. Rypina,[1] M. G. Brown,[1] F. J. Beron-Vera,[1] H. Koçak,[2] M. J. Olascoaga,[1] and I. A. Udovydchenkov[1]

[1]*RSMAS/AMP, University of Miami, 4600 Rickenbacker Causeway, Miami, Florida, 33149, USA*

[2]*Departments of Computer Science and Mathematics, University of Miami, Coral Gables, Florida, 33124, USA*

(Received 21 September 2006; published 8 March 2007)

Hamiltonian systems that locally violate the twist condition arise in many applications. Numerical simulations reveal that, when systems of this type are perturbed, the degenerate or nontwist tori are remarkably stable. This phenomenon, which we refer to as strong Kolmogorov-Arnold-Moser (KAM) stability, is shown to be linked to very small resonance widths near degenerate tori. Quantitative estimates of degenerate resonance widths are derived and bifurcations of degenerate resonances are described. Strong KAM stability leads to robust transport barriers, which are important in all of the many applications in which Hamilitonians with the nontwist property arise.

DOI: 10.1103/PhysRevLett.98.104102 PACS numbers: 05.45.Ac, 45.20.Jj, 47.27.ed, 47.52.+j

The work reported here was motivated by a desire to understand the mechanism by which ozone-depleted air is trapped within the ozone hole [1]. In that problem the atmospheric flow is assumed to be two dimensional and incompressible. The fluid parcel trajectory equations of motion then have Hamiltonian form. After transforming to action-angle (I, θ) variables the essential ingredients of the ozone hole problem are the following. The Hamiltonian $H(I, \theta, t)$ can be decomposed as

$$H(I, \theta, t) = H_0(I) + \varepsilon H_1(I, \theta, \sigma t) \tag{1}$$

where H_1 is $2\pi/\sigma$ periodic in t. Each unperturbed ($\varepsilon = 0$) torus is labeled by its action I; the corresponding frequency is $\omega(I) \equiv dH_0/dI = H_0'(I)$. Under perturbation, at the perimeter of the ozone hole there is a thin band of very robust invariant tori in the vicinity of the torus that violates the twist or nondegenerate property $\omega'(I) \neq 0$. These invariant tori serve as a transport barrier between the interior and exterior of the ozone hole. The ozone hole problem will not be further discussed here. Rather, we consider the generic problem defined by Eq. (1) focusing on the stability of degenerate tori, i.e., tori that satisfy $\omega'(I) = 0$. We focus on the generic Hamiltonian problem because the same problem arises in many applications including simple mechanical systems [2], charged particle dynamics in magnetic fields [3], celestial dynamics [4], stellar pulsations [5], plasma physics [6], underwater acoustics [7], and transport and mixing in the ocean and atmosphere [1,8]. We show that, owing to small resonance widths near degenerate tori under perturbation, robust transport barriers are found near such tori under typical conditions. The resulting transport barriers are important in all of the applications mentioned.

The technical results presented below can be summarized as follows. The KAM (Kolmogorov-Arnold-Moser) theorem [9–11] guarantees that, provided certain conditions are met, many of the unperturbed tori associated with the system described by $H_0(I)$ survive under perturbation. Torus destruction is caused by the excitation of resonances when the ratio of the frequency $\omega(I)$ of the motion on the unperturbed torus to the forcing frequency σ is rational. Associated with each resonance is a characteristic width. Resonance widths are important because overlapping resonances lead to the destruction of the unperturbed tori with I values between those of the resonant tori [12–14]. All variants of the KAM theorem [9–11] require that a nondegeneracy condition be satisfied. The simplest such condition, due originally to Kolmogorov [9], is $\omega'(I) \neq 0$. This condition guarantees that for sufficiently small ε resonances are isolated. Nondegenerate resonance widths scale like $\Delta\omega \sim \varepsilon^{1/2}$. The Rüssmann [10] form of the KAM theorem employs a weaker nondegeneracy condition. Transforming (1) to an autonomous 2 degree-of-freedom system reveals [1] that the Rüssmann nondegeneracy condition is satisfied in domains that include points where $\omega'(I) = 0$, i.e., that are degenerate in the Kolmogorov sense. Related results for area-preserving maps are discussed in [15]. We show below that the degenerate resonance widths scale like $\Delta\omega \sim \varepsilon^{j/(j+1)}$ where $j = 2, 3, \ldots$ is the number of nondegenerate resonances that coalesce at the degenerate point. We refer to j below as the order of the degeneracy. For small ε degenerate resonance widths are generally smaller than nondegenerate resonant widths. This leads to the phenomenon that we refer to as "strong KAM stability" and very robust transport barriers. An example will be given below.

Mathematical details underlying the phenomenon of strong KAM stability will now be given. Consider a system described by Eq. (1) where I and θ evolve according to $\dot{I} = -\partial H/\partial\theta$, $\dot{\theta} = \partial H/\partial I$. The perturbation $H_1(I, \theta, \sigma t)$ is 2π periodic in θ and $2\pi/\sigma$ periodic in t, so H_1 can be expanded in a Fourier series, $H_1(I, \theta, \sigma t) = \sum_{m,n=-\infty}^{\infty} V_{nm}(I)\cos(n\theta - m\sigma t + \phi_{nm})$ where the ϕ_{nm}'s are phases. The equations of motion are

$$\dot{I} = \varepsilon \sum_{m,n=-\infty}^{\infty} nV_{nm}(I)\sin(n\theta - m\sigma t + \phi_{nm}), \tag{2}$$

$$\dot{\theta} = \omega(I) + \varepsilon \sum_{m,n=-\infty}^{\infty} nV_{nm}'(I)\cos(n\theta - m\sigma t + \phi_{nm}). \tag{3}$$

In the $\varepsilon = 0$ limit, solutions are $I(t) = \text{const}$, $\theta(t) = \text{const} + \omega(I)t$, and the motion is periodic. Let $\omega^{(j)}(I_0)$ denote the jth derivative of $\omega(I)$ at $I = I_0$. In anticipation of our analysis of a jth order degeneracy, we shall assume that $\omega(I)$ satisfies $\omega^{(j-1)}(I_0) = 0$, $\omega^{(j)}(I_0) \neq 0$ for some integer $j \geq 2$ and some I_0 in the I domain of interest. Also, we assume that ε is small and σ is an adjustable parameter that is close to the value σ_0 at which the resonance condition $n\omega(I_0) = m\sigma_0$ is satisfied. Following [13,16], the oscillating nonresonant terms in Eqs. (2) and (3) will be omitted and $V_{nm}(I)$ will be replaced by the resonant value $V_{nm}(I_0)$ in the approximate analysis that follows. Let $\psi = n\theta - m\sigma t + \phi_{nm}$ corresponding to the resonant (n, m) pair. Then, noting that $\dot{\psi} = n\dot{\theta} - m\sigma$, and expanding $\omega(I)$ in a Taylor series about I_0, with $\delta I = I - I_0$, yields the following approximate autonomous system in the vicinity of the resonant level:

$$\delta\dot{I} = \varepsilon n V_{nm}(I_0)\sin\psi, \tag{4}$$

$$\dot{\psi} = n\left[\omega(I_0) + \omega'(I_0)\delta I + \cdots + \omega^{(j-2)}(I_0)\frac{(\delta I)^{j-2}}{(j-2)!} + \omega^{(j)}(I_0)\frac{(\delta I)^j}{j!}\right] - m\sigma. \tag{5}$$

An $O(\varepsilon)$ term in Eq. (5) has been omitted. The justification for this is that it will be shown below [Eq. (10)] that δI scales like $\varepsilon^{1/(j+1)}$. For convenience we introduce the notation $\Omega_i = \omega^{(i)}(I_0)/i!$, $i = 0, 1, \ldots, j-2$. Equations (4) and (5) define a Hamiltonian system

$$\delta\dot{I} = -\partial\tilde{H}/\partial\psi, \qquad \dot{\psi} = \partial\tilde{H}/\partial\delta I, \tag{6}$$

with Hamiltonian

$$\tilde{H}(\delta I, \psi) = n\left[\Omega_0\delta I + \Omega_1\frac{(\delta I)^2}{2} + \cdots + \omega^{(j)}(I_0)\frac{(\delta I)^{j+1}}{(j+1)!}\right] - m\sigma\delta I + \varepsilon n V_{nm}(I_0)\cos\psi. \tag{7}$$

Consistent with Eq. (7) is the expansion

$$\omega(\delta I; \mathbf{\Omega}) = \Omega_0 + \Omega_1\delta I + \cdots + \Omega_{j-2}(\delta I)^{j-2} + \omega^{(j)}(I_0)\frac{(\delta I)^j}{j!}. \tag{8}$$

In the following we will consider separately (1) degenerate reonance widths and (2) bifurcations of degenerate resonances.

First, we estimate the width of a degenerate resonance of order j. At such a resonance $\sigma = \sigma_0 = \frac{n}{m}\Omega_0$ and $\Omega_1 = \Omega_2 = \ldots = \Omega_{j-2} = 0$, so the Hamiltonian (7) reduces to

$$\tilde{H}(\delta I, \psi) = n\omega^{(j)}(I_0)\frac{(\delta I)^{j+1}}{(j+1)!} + \varepsilon n V_{nm}(I_0)\cos\psi. \tag{9}$$

Level surfaces of $\tilde{H}$ in the phase plane $(\delta I, \psi)$ have qualitatively different features depending on whether j is odd or even. An example of each type is shown in Fig. 1. In these systems trajectories are divided by a separatrix into two types: trajectories trapped in the resonance region and trajectories external to the resonance region. It is natural to define the resonance width as the width of the trapped

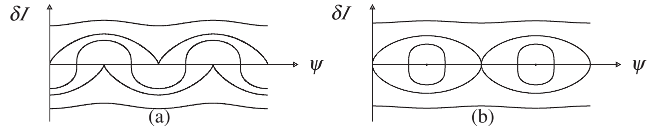

FIG. 1. Level surfaces of $\tilde{H}(\delta I, \psi)$ defined by Eq. (9) in the phase plane $(\psi, \delta I)$ for $j = 2$ (a) and $j = 3$ (b).

region. This is the maximum δI excursion of the separatrix,

$$\Delta I = \left(\frac{2\varepsilon|V_{nm}(I_0)|(j+1)!}{|\omega^{(j)}(I_0)|}\right)^{1/(j+1)}. \tag{10}$$

The corresponding frequency width is

$$\Delta\omega = |\omega^{(j)}(I_0)|\frac{(\Delta I)^j}{j!} = |\omega^{(j)}(I_0)|^{1/(j+1)}\frac{(2\varepsilon|V_{nm}(I_0)|(j+1)!)^{1/(j+1)}}{j!}. \tag{11}$$

Although our focus is on degenerate $(j \geq 2)$ resonance widths, Eqs. (10) and (11) apply to the nondegenerate case $j = 1$ as well. The ε scaling associated with ΔI, Eq. (10), was previously derived [17] using different arguments. Our focus is on $\Delta\omega$, Eq. (11), as this width controls whether neighboring resonances overlap [12–15]. Number-theoretic issues relating to n and m (the degree of rationality of n/m) are well known [18] and will not be discussed here.

The scaling $\Delta\omega \sim \varepsilon^{j/(j+1)}$ predicted by Eq. (11) leads, when ε is small and j is large, to small resonance widths and strong KAM stability, as illustrated using $j = 2$ in Fig. 2. In that figure, Poincaré sections for two systems with $H(I, \theta, t) = H_0(I) + \varepsilon H_1(I, \theta, \sigma t)$ are shown. The structure and strength of the perturbation term $\varepsilon H_1(I, \theta, \sigma t)$ is the same in both cases, but $H_0(I)$ is not. In one case $\omega(I)$ is linear. In the other case $\omega(I)$ is cubic and there are two isolated $j = 2$ degeneracies. The same $\omega(I)$ domain is present for both choices of $H_0(I)$, so the same resonances are excited in both cases. The resonance widths are different, however, and, consistent with

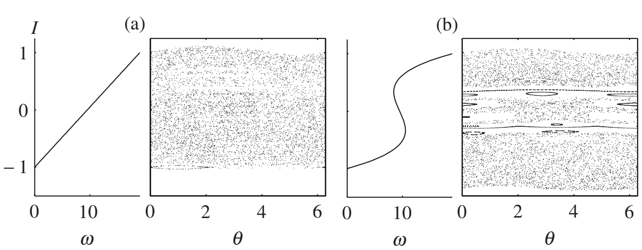

FIG. 2. Frequency structure $\omega(I)$ and the corresponding Poincaré section for the system with Hamiltonian $H_0(I) + \varepsilon H_1(I, \theta, \sigma t)$ for two choices of $H_0(I)$: (a) linear $\omega(I)$; (b) cubic $\omega(I)$. In both cases $\varepsilon = 0.026$ and $H_1(I, \theta, \sigma t) = \sum_{i=1}^{19}\cos(\sigma_i t)\cos(I + \theta)$, where the 19 forcing frequencies are commensurable and lie in the ω domain plotted.

Eq. (11), this leads to strong stability of the tori in the vicinity of the degenerate tori in the system with cubic $\omega(I)$.

We now consider bifurcations of degenerate resonances. σ and Ω_i, $i = 1, 2, \ldots, j-2$, will now be treated as adjustable parameters. In contrast, we shall assume that $\omega^{(j)}(I)$ has no zeros in the domain of interest and treat $\omega^{(j)}(I_0)$ as a constant rather than an adjustable parameter. This assumption allows us to approximate $\omega(I)$ as a finite order polynomial; other, more rigorous, arguments can be used to justify the same approximation [19]. The resonance condition can be written $\omega(\delta I; \boldsymbol{\Omega}) = \frac{m}{n}\sigma$ and the condition defining a degenerate resonance is $\partial\omega(\delta I; \boldsymbol{\Omega})/\partial\delta I = 0$. (A partial derivative is used here to emphasize that the Ω_i's are held constant when the derivative is taken.) Together with Eq. (11) these two conditions define Legendre singularities [19,20] in the $(j-1)$-dimensional control parameter space $(\Omega_0 - \frac{m}{n}\sigma, \Omega_1, \ldots, \Omega_{j-2})$. These singularities belong to the cuspoid family and have well-known forms (fold for $j = 2$, cusp for $j = 3$, swallowtail for $j = 4$, etc.). The singular structure associated with the fold and cusp in control parameter space and selected associated forms of $\omega(\delta I; \boldsymbol{\Omega})$ are shown in Fig. 3. Note that j is the number of nondegenerate resonances that coalesce at the point $\sigma = \sigma_0 = \frac{n}{m}\Omega_0$, $\Omega_1 = \Omega_2 = \ldots = \Omega_{j-2} = 0$. Additional numerical simulations based on the fold ($j = 2$) are provided below; extensions to higher dimensional structures ($j = 3, 4, \ldots$) are straightforward. Two points regarding bifurcations of degenerate resonances should be emphasized. First, in control parameter space high order structures unfold into a configuration of lower order structures; the cusp unfolds into two fold lines, for example. Second, structural stability of a jth order degeneracy requires that it reside in a control parameter space of dimension $j-1$ or higher. This implies, for instance, that an experimental apparatus designed to generate a jth order degeneracy must in general have $j-1$ controls. [Structurally unstable problems sometimes arise in applications. Motion in the structurally unstable system corresponding to (1) with $H_0(I) = \omega_0 I$, $\omega(I) = \omega_0 = \text{const}$, has been extensively studied [3,21].]

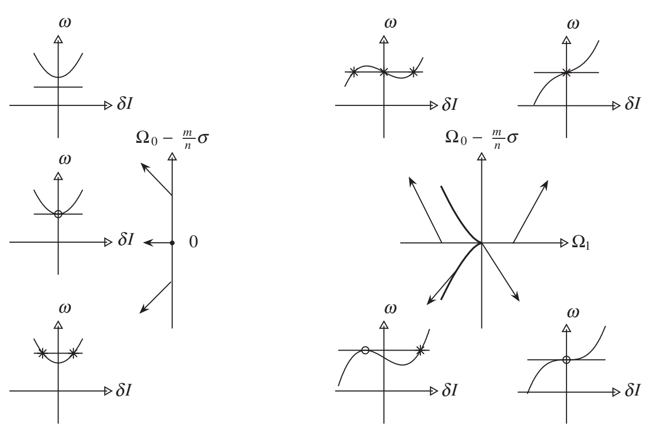

FIG. 3. Legendre singularities in the $(j-1)$-dimensional control parameter space and, at selected locations in that space, associated intersections of the line $m\sigma = n\omega$ with the curve $\omega(\delta I; \boldsymbol{\Omega})$: (left) fold, $j = 2$; (right) cusp, $j = 3$. Open circles identify excited degenerate resonances.

Associated with the singular structures (Legendre singularities) in control parameter space $(\Omega_0 - \frac{m}{n}\sigma, \Omega_1, \ldots, \Omega_{j-2})$ are bifurcations in the phase plane $(\delta I, \psi)$. Consider the simplest degenerate case corresponding to the fold. For this system $\omega(\delta I; \boldsymbol{\Omega})$ and $\tilde{H}(\delta I, \psi)$ are defined by Eqs. (7) and (8), respectively, with $j = 2$. The set of singular (degenerate) points that satisfy $\omega(\delta I; \Omega_0) = \frac{m}{n}\sigma$, $\partial\omega(\delta I; \Omega_0)/\partial\delta I = 0$ is the point $\frac{m}{n}\sigma = \Omega_0$ or $\sigma = \sigma_0$, as indicated in Fig. 3. Level surfaces of $\tilde{H}(\delta I, \psi)$ in the phase plane for this system using five different values of the forcing frequency σ that span the degenerate value σ_0 are shown in Fig. 4. For simplicity we have chosen to focus on the $n = m = 1$ resonance in this figure. Assuming $\omega^{(2)}(I_0) > 0$, as shown in Fig. 3 (left), two resonances are excited when the forcing frequency $\sigma > \sigma_0 = \Omega_0$. For large $\sigma - \sigma_0$ two nonoverlaping resonances are present [Fig. 4(a)]. At a critical value of $\sigma > \sigma_0$, a reconnection of separatrices takes place [Fig. 4(b)]; at this critical value two hyperbolic heteroclinic chains [Fig. 4(a)] are transformed to two hyperbolic homoclinic chains [Fig. 4(c)]. When the forcing frequency σ reaches the value σ_0 the degenerate resonance is excited [Fig. 4(d)]. For $\sigma < \sigma_0$ the 1:1 resonance is not excited [Fig. 4(e)]. Related results for both the fold and the cusp are presented in [22].

The preceding analysis is based on the approximate autonomous system (6) and (7). We now demonstrate the validity of this approximate analysis by showing that its predictions are in good agreement with simulations based on the nonautonomous system (1). For this purpose we consider the nonautonomous system $H(I, \theta, \sigma t) = \sin I + I + \varepsilon\cos(\sigma t)\cos\theta$ for which $H_0(I) = \sin I + I$ has a second-order ($j = 2$) degeneracy at $I_0 = 0$. In response to the periodic forcing some resonances are excited. In Fig. 5 the forcing frequency σ is chosen to be close to that of the frequency of the degenerate torus $\omega(I_0) = \Omega_0 = 2$, so that the 1:1 resonance is excited. Gradually increasing the forcing frequency from $\sigma = 1.3$ (corresponding to two nondegenerate resonances far away from the degenerate level) to $\sigma = 2$ (exact degenerate resonance of second order), results in the excitation of resonances closer and

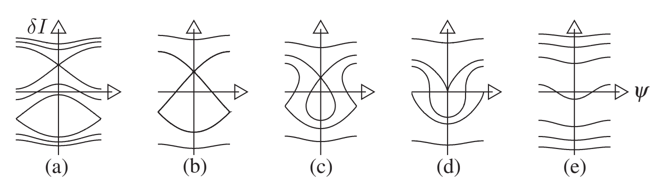

FIG. 4. Level surfaces of $\tilde{H}(\delta I, \psi)$ defined by Eq. (7) with $j = 2$, $\omega^{(2)}(I_0) > 0$, $n = m = 1$, for five choices of σ, decreasing montonically from (a) to (e). In (a), (b), and (c) $\sigma > \Omega_0$; in (d) $\sigma = \Omega_0$; in (e) $\sigma < \Omega_0$.

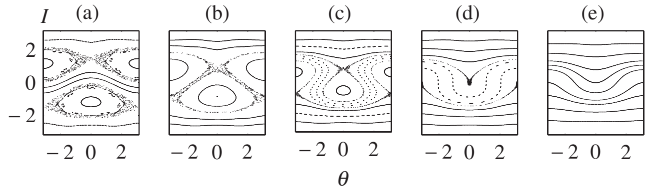

FIG. 5. Poincaré sections for the system described by Eq. (1) with $H_0(I) = I + \sin I$, $H_1(I, \theta, \sigma t) = \cos(\sigma t)\cos\theta$, $\varepsilon = 0.5$, for five choices of σ: (a) $\sigma = 1.3$; (b) $\sigma = 1.6$; (c) $\sigma = 1.79$; (d) $\sigma = 2.0$; (e) $\sigma = 2.23$.

closer to the degenerate level. A further increase of the forcing frequency results in the nonexcitation of the dominant 1:1 resonance. Although, for each choice of σ, many resonances are excited, the dominant resonance is the 1:1 resonance, and good agreement between this figure and Fig. 4 is seen. Because Fig. 5 does not make use of any of the approximations we have introduced, the good qualitative agreement between Figs. 4 and 5 serves to illustrate the validity of the approximate analysis that we have made use of.

In this Letter we have shown that resonance widths $\Delta\omega$ in the vicinity of degenerate tori are generally narrower than those in the vicinity of nondegenerate tori. Although noninvertibility of the frequency map $\omega(I)$ leads to difficulties in the proof of the KAM theorem (that Rüssmann [10] has overcome), we have encountered no such difficulties because at locations where $\omega'(I)$ has isolated zeros both ΔI and $\Delta\omega$ are well defined. As a result of generally small resonance widths $\Delta\omega$ near degenerate tori, resonances near degenerate tori are less likely to overlap, and tori in the vicinity of degenerate tori are generally more stable than those in the vicinity of nondegenerate tori. We have referred to this phenomenon as strong KAM stability. Tori that survive under perturbation serve as transport barriers. Owing to strong KAM stability, degenerate tori are associated with robust transport barriers. Bifurcations of degeneracies have been described. Numerical simulations, including but not limited to those presented in Figs. 2 and 5, support the analysis that we have presented and illustrate the importance of strong KAM stability and the associated robust transport barriers.

This work was supported by the National Science Foundation, Grant No. GMC0417425, and Code 321 of the Office of Naval Research.

[1] I. I. Rypina, M. G. Brown, F. J. Beron-Vera, H. Kocak, M. J. Olascoaga, and I. A. Udovydchenkov, J. Atmos. Sci. (to be published).
[2] J. Koiller, R. Markarian, S. Olison-Kamphorst, and S. P. de Carvalho, Nonlinearity **8**, 983 (1995); J. Koiller, R. Markarian, S. Olison-Kamphorst, and S. P. de Carvalho, J. Stat. Phys. **83**, 127 (1996).
[3] G. M. Zaslavskii, M. Yu. Zakharov, R. Z. Sagdeev, D. A. Usikov, and A. A. Chernikov, Sov. Phys. JETP **64**, 294 (1986).
[4] W. T. Kyner, Mem. Am. Math. Soc. **81**, 1 (1968).
[5] A. Munteanu, E. Petrisor, E. Garcia-Berro, and J. Jose, Commun. Nonlinear Sci. Numerical Simul. **8**, 355 (2003).
[6] G. A. Oda and I. L. Caldas, Chaos Solitons Fractals **5**, 15 (1995); R. Balescu, Phys. Rev. E **58**, 3781 (1998); W. Horton, H. B. Park, J. M. Kwon, D. Strozzi, P. J. Morrison, and D. I. Choi, Phys. Plasmas **5**, 3910 (1998); K. Ullmann and I. L. Caldas, Chaos Solitons Fractals **11**, 2129 (2000); E. Petrisor, J. H. Misguich, and D. Constantinescu, Chaos Solitons Fractals **18**, 1085 (2003); P. J. Morrison, Phys. Plasmas **7**, 2279 (2000).
[7] M. G. Brown, J. A. Colosi, S. Tomsovic, A. L. Virovlyansky, M. Wolfson, and G. M. Zaslavsky, J. Acoust. Soc. Am. **113**, 2533 (2003); I. P.Smirnov, A. L. Virovlyansky, and G. M. Zaslavsky, Phys. Rev. E **64**, 036221 (2001).
[8] D. del-Castillo-Negrete and P. J. Morrison, Phys. Fluids A **5**, 948 (1993).
[9] A. N. Kolmogorov, Dokl. Akad. Nauk SSSR **98**, 525 (1954); English translation in G. Casati and J. Ford, Lect. Notes Phys. **93**, 51 (1979).
[10] H. Rüssmann, in *Number Theory and Dynamical Systems*, London Math. Soc. Lect. Notes Series (Cambridge University, Cambridge, England, 1989), pp. 5–18.
[11] V. I. Arnold, Russ. Math. Surv. **18**, 9 (1963); A. D. Bruno, Sov. Math. Dokl. **45**, 221 (1992).
[12] B. V. Chirikov, Phys. Rep. **52**, 263 (1979).
[13] B. V. Chirikov and G. M. Zaslavsky, Sov. Phys. Usp. **14**, 549 (1972).
[14] A. G. Lichtenberg and M. A. Lieberman, *Regular and Stochastic Motion* (Springer, New York, 1983).
[15] C. Simo, Reg. Chaotic Dyn. **3**, 180 (1998); A. Delshams and R. de la Llave, SIAM J. Math. Anal. **31**, 1235 (2000).
[16] G. Zaslavsky, *Chaos in Dynamic Systems* (Harwood Academic Publishers, NY, 1985); S. S. Abdullaev, *Chaos and the Dynamics of Rays in Waveguide Media* (Gordon and Breach, New York, 1993), Vol. 6.
[17] A. D Morozov, Chaos **12**, 539 (2002); A. D. Morozov and L. P. Shilnikov, Prikl. Mat. Mekh. **47**, 385 (1983).
[18] J. M. Greene, J. Math. Phys. (N.Y.) **20**, 1183 (1979).
[19] V. I. Arnold, S. M. Gusein-Zade, and A. N. Varchenko, *Singularities of Dierentiable Maps, Vol. I*, Monographs in Mathematics Vol. 82 (Birkhauser, Boston, 1985).
[20] M. Brown and F. Tappert, Geophys. J. R. Astron. Soc. **88**, 217 (1987).
[21] G. M. Zaslavsky, R. Z. Sagdeev, D. A. Usikov, and A. A. Chernikov, *Weak Chaos and Quasi-Regular Patterns* (Cambridge Nonlinear Science Series, New York, 1991).
[22] H. R. Dullin, A. V. Ivanov, and J. D. Meiss, Physica (Amsterdam) **215D**, 175 (2006).